Talanta 144 (2015) 1044–1051

Contents lists available at ScienceDirect

Talanta

journal homepage: www.elsevier.com/locate/talanta

Development of N-ferrocenyl(benzoyl)amino-acid esters stationary phase for high performance liquid chromatography

Xiaohua Zhou [a], Xiaole Li [b], Aijuan Cao [a], Lijun Qiao [a], Ajuan Yu [a,*], Shusheng Zhang [a,*], Yangjie Wu [a]

[a] The College of Chemistry and Molecular Engineering, Key Laboratory of Chemical Biology and Organic Chemistry of Henan, Zhengzhou University, Zhengzhou 450052, PR China
[b] Metallurgical and Chemical Department, Jiyuan Vocational and Technical College, Jiyuan 459000, PR China

ARTICLE INFO

Article history:
Received 14 May 2015
Received in revised form
18 July 2015
Accepted 23 July 2015
Available online 26 July 2015

Keywords:
Ferrocene stationary phase
High performance liquid chromatography
Retention mechanism
Organophosphorus pesticide

ABSTRACT

A new stationary phase for high-performance liquid chromatography was prepared by covalently bonding N-ferrocenyl(benzoyl)amino-acid esters (L^1) onto silica gel using 3-aminopropyltriethoxysilane as coupling reagent. The structure of new material was characterized by infrared spectroscopy, elemental analysis and thermogravimetric analysis. The chromatographic behavior of the phase was illustrated in reversed-phase (RP) and normal-phase (NP) modes using polycyclic aromatic hydrocarbons (PAHs), aromatics positional isomers, amines, 5-nitroimidazoles, organophosphorus pesticides and phenols as probes. Multiple mechanisms including hydrophobic, hydrogen bonding, π–π, dipole–dipole, charge-transfer and acid–base equilibrium interactions are involved. Thus, multi-interaction mechanisms and mixed-mode separation of the new phase can very likely guarantee its excellent chromatographic performance for the analysis of complex samples. The L^1 AminoSil column was successfully employed for the analysis of organophosphorus pesticides in vegetable.

1. Introduction

The grafting on silica gel of electron acceptor molecules bearing transition metal metallocenes [1–5] is another investigated field of research [1,5]. In recent years, the ferrocene-bonded stationary phase has attracted considerable attention in liquid chromatography due to its varieties of separation mechanisms, including hydrophobic, hydrogen bonding, π–π, dipole–dipole and charge-transfer interactions [6–10]. Complexing properties of ferrocene receptors depend mainly on the type and arrangement of binding site. Ferrocene complexes have been demonstrated to be strong receptors with polynuclear π-aromatic hydrocarbons (PAHs), aniline derivatives and so on, which probably associate with the metallocenes, phenyl ring, amine and amide hydrogen atoms packed in the ferrocene complexes via hydrophobic, π–π interactions and hydrogen bonding. Delville group [6,7] and Zuo group [8,9] demonstrated that the stationary-phase, bonded with covalently linking ferrocene of so-called "organometallic/inorganic" hybrid materials, exhibited high selectivity towards the separation of alkylbenzenes, halobenzenes, PAHs and aniline derivatives under normal-phase (NP) or reversed-phase (RP) conditions.

The retention of solutes on the stationary phase may involve a variety of interaction mechanisms, such as hydrophobic, π–π, hydrogen bonding and charge-transfer interactions in high performance liquid chromatography (HPLC). Our previous work [10] described the synthesis and characterization of a 4-ferrocenylbenzoyl chloride-bonded stationary phase for HPLC, which was highly selective towards various compounds, such as PAHs, monosubstituted benzenes, ferrocenyl derivatives, aromatic amines, pyrazine derivatives, drug intermediate pyrrole isomers and sulfonamides. The two cyclopentadienyl carbon rings, phenyl ring and amido group in this bonded stationary phase might serve to increase the selectivity of chromatographic separation. As a result, the stationary phases utilizing a multimode retention mechanism have been proposed to achieve the desired improvement in the selectivity of separation of specific solutes and can offer more potential than classical reversed-phase (RP) or normal-phase (NP) chromatography [11–13]. Therefore, the exploitation of new functional ferrocene molecules and the utilization of them as selectors in chromatography separation have become one of the hotspots in chromatographic science.

N-ferrocenyl(benzoyl)amino-acid esters (L^1) is a typical ferrocene compound and has been used for electrochemical anion recognition [14]. No effort has been made to their chromatographic applications. It has unique interaction sites as a chromatographic ligand, for instance hydrophobic alkyl chains (hydrophobic

* Corresponding authors. Fax: +86 371 6776 3224.
E-mail addresses: yuajuan@zzu.edu.cn (A. Yu), zsszz@126.com (S. Zhang).

http://dx.doi.org/10.1016/j.talanta.2015.07.063
0039-9140/

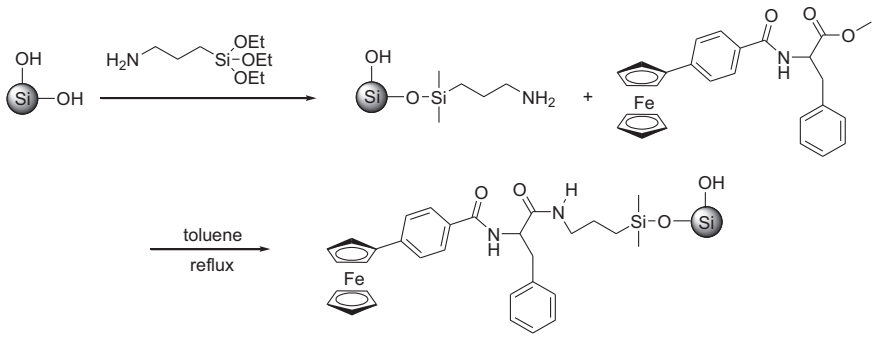

Fig. 1. Schemes demonstrating the synthesis of L[1]AminoSil stationary phase.

interaction), phenyl rings (π–π interaction), polar phenylalanine groups (hydrogen bonding and dipole–dipole interaction) which structurally distinct from the presented ferrocene phases [6–10]. It was anticipated that the phenyl rings, amino groups and alkyl chains in this L^1 might serve to increase selectivity of chromatographic separation. It would be interesting to associate the ferrocene ligand as stationary phase (L^1AminoSil) for HPLC. The paper showed for the first time the use of N-ferrocenyl(benzoyl)amino-acid esters (L^1) attached on the silica surface for separation of PAHs, aromatics positional isomers, amines, 5-nitroimidazoles, organophosphorus pesticides and phenols in HPLC. As a consequence of its distinct structure binding sites, the bonded material was a true multimode phase that, depending on the elution conditions and the characteristics of the selected solutes, could be operated in a variety of chromatographic modes, such as RP and NP modes. A method for the determination of organophosphorus pesticides in vegetable sample was set up by using our newly prepared column.

2. Experimental

2.1. Apparatus and materials

HPLC was performed by using an Agilent 1260 series system equipped with a 1200 model quaternary pump, a 1260 Infinity DAD detector and a G1316A model thermostatic column compartment. Elemental analysis was performed on a Flash EA1112 elemental analyzer (Thermo Electron Corporation). Thermal gravimetric analysis (TGA) was carried out using a Shimadzu DT-40 thermal analyzer, and the analysis was performed from 40 °C to 600 °C at a heating rate of 10 °C per minute in nitrogen atmosphere with a gas flow rate of 20 mL min^{-1}.

Silica gel (particle size of 5 μm, pore size of 100 Å and specific surface area of 300 m^2 g^{-1}) was provided by Lanzhou Institute of Chemical and Physics of CAS (Lanzhou, China). 3-aminopropyltriethoxysilane was purchased from Aladdin Industrial Corporation (Shanghai, China). Methanol and acetonitrile of HPLC grade were purchased from Dikma (Beijing, China). All other chemicals and solvents used in this study were of analytical grade unless specially mentioned. Water used was obtained from Milli-pore water purification system.

2.2. Preparation of L1AminoSil stationary phase

2.2.1. Synthesis of 3-aminopropyl bonded silica gel

Activated silica gel (5.0 g) and anhydrous toluene (80 mL) were added to a flask equipped with a gas inlet valve and a reflux condenser. After the addition of 3-aminopropyl trimethoxysilane (10 mL) and triethylamine (0.15 mL), the mixture was magnetically stirred and refluxed at 115 °C under nitrogen atmosphere for 48 h. Then, the mixture was cooled to room temperature and filtered. The residue was washed in sequence with toluene, acetone and distilled water. Finally, the product of 3-aminopropyl bonded silica gel (ABS) was dried under vacuum at 100 °C for 8 h and used as a precursor in the following reaction.

2.2.2. Synthesis of N-{para-(ferrocenyl)benzoyl}-phenyl-alanine methyl ester (L^1)

N-{*para*-(ferrocenyl)benzoyl}-phenyl-alanine methyl ester was prepared by the following literature procedure [14]. 4-Ferrocenylbenzoyl carboxylic acid (2.6320 g, 8.6 mmol) and N-hydroxy benzotriazole (1.3 g, 9.5 mmol) were dissolved in dry DMF and then cooled to 0 °C under nitrogen atmosphere. Solution of dicyclohexylcarbodiimide (DCC) (2.1 g, 10.4 mmol) in dichloromethane was added and the reaction mixture was stirred at 0 °C for an hour. Then phenylalanine methyl ester hydrochloride (1.712 g, 9.5 mmol), triethylamine (1.4 mL, 10.4 mmol) were added and the mixture was stirred for another 24 h at room temperature. After filtration and concentration, the crude product was dissolved in dichloromethane and organic layer was washed with 1 N HCl (3 × 30 mL), 10% $NaHCO_3$ (3 × 30 mL) and brine (26% NaCl) (30 mL), respectively. Organic layer was dried over anhydrous sodium sulfate and concentrated in reduced pressure. The crude product was purified on a silica gel column (100–200 mesh) with a mixture of dichloromethane and methanol (97:3), yielding pure product as a red crystal, characterized by comparison with literature data (^{1}H NMR and ^{13}C NMR spectra). The yield was 60%.

2.2.3. Synthesis of L^1AminoSil stationary phase

Fig. 1 shows the synthesis process of the new L[1]AminoSil stationary phase. Details of the bonding procedure are as follows: a mixture of N-{*para*-(ferrocenyl)benzoyl}-phenyl-alanine methyl ester (1.50 g), ABS (3.0 g) and toluene (75 mL) was refluxed at 115 °C for 12 h under nitrogen atmosphere. After completion of the reaction, the product was filtered and washed in sequence with N, N-dimethyl aniline, toluene, acetone, methanol and distilled water. Subsequently, the L[1]AminoSil stationary phase was dried under vacuum at 50 °C for 24 h before packing and characterization.

The prepared L[1]AminoSil was packed into a steel tube column (150 mm × 4.6 mm i.d.) by using a packing machine (Kerui Tech. Co. Ltd., Dalian, China) according to a slurry packing procedure by using tetrachloromethane/isopropanol (95:5, v/v) as the displacing agent (40 MPa, 30 min).

3. Results and discussion

3.1. Characterization of L^1AminoSil stationary phase

A comparison of ABS and L[1]AminoSil IR spectra showed that new absorptions appeared at 1608, 1543 and 1398 cm^{-1}, which

corresponded to the groups of benzene rings (C–H). The chemical grafting of the ferrocene units was pointed out by the new stretching bands due to C–H vibrations of the cyclopentadienyl ligands (2936 cm^{-1}) and the presence of the amide bands (NCO) at 1646 cm^{-1} and 1513 cm^{-1}. The large bands centered on 1112 cm^{-1}, 805 cm^{-1} were assigned to the Si–O and Si–O–Si stretching modes, respectively. These differences suggest that the molecular N-{*para*-(ferrocenyl)benzoyl}-phenyl-alanine methyl ester was successfully immobilized onto ABS.

Quantitative determination of the packing material was achieved by elemental analysis. Elemental analysis results showed that the content of C, H and N in ABS was 4.49%, 1.08% and 1.02%, respectively; the C, H and N in L^1AminoSil was 8.80%, 1.69% and 1.27%, respectively. The bonding amount of L^1 was about 133 μmol g^{-1} based on the change of carbon content. Both the IR spectra and the elemental analysis results indicate successful preparation of L^1AminoSil.

TG analysis curve showed that the weight loss temperature of L^1AminoSil was higher than 272 °C, indicating the packing material possessed better thermal stability and chemical stability. The total weight loss was 9.58% for L^1AminoSil in the temperature range of 40–600 °C, which indicated the stationary phase had good thermal stability below 250 °C.

3.2. Chromatographic separations

3.2.1. Separation of PAHs

In this section, the chromatographic retention behaviors of five PAHs (benzene, biphenyl, phenanthrene, chrysene and perylene) were investigated on the L^1AminoSil stationary phase. Fig. 2 shows the typical chromatograms on both L^1AminoSil and Octadecylsilyl (ODS), and Table 1 listed their log $K_{o/w}$ values (the log octanol–water partition coefficient). It can be seen from Fig. 2 and Table 1 that the elution order of analytes on L^1AminoSil was the same as that on ODS, the k values increased with the increase of log $K_{o/w}$ values. Meanwhile, the k values of five PAHs linearly declined with increase of methanol content in the mobile phase (Fig. 3). These results were in accordance with reversed-phase separation mechanism, and indicated that hydrophobic interaction between the L^1AminoSil stationary phase and PAHs played an important role in the separation. On the other hand, the retention times of PAHs on L^1AminoSil stationary phase were extremely shorter than those on ODS, which indicated that the hydrophobic interaction on L^1AminoSil was weaker than the latter. In addition, this was presumably due to the strong polarity of mobile phase in RP mode, which might seriously weaken the π–π interactions between the solutes and the bonded phase. But the former had advantage in the rapid analysis of the above mentioned nonpolar aromatics.

3.2.2. Separation of aromatic compounds

In this section, the separations for some aromatic compounds with different polar and nonpolar character were individually investigated on L^1AminoSil stationary phase. Retention capacity factors (k) of the analytes were calculated under the optimized chromatographic conditions, and listed in Table 2. Among them, aromatic amines in each group were separated to baseline on our new ferrocene stationary phase under the optimized chromatographic conditions in NP mode.

In contrast with our previous study of 4-ferrocenylbenzoyl chloride-bonded stationary phase (Fc–SiO_2), one goal of this work was mainly to evaluate the chromatographic performance of the new phase after the introduction of phenylalanine molecule between the polar amido function and ferrocene group. In the new ferrocene phenyl-alanine methyl ester, the strong conjugation system due to phenyl ring being conjugated with their adjacent carbonyl group and another phenyl ring in phenyl-alanine unit made the new ferrocene have stronger delocalization π electrons than the previous one. Thus, the stronger π–π interaction than the former could be predicated, and it would let us explore the practical applications of the new L^1AminoSil stationary phase.

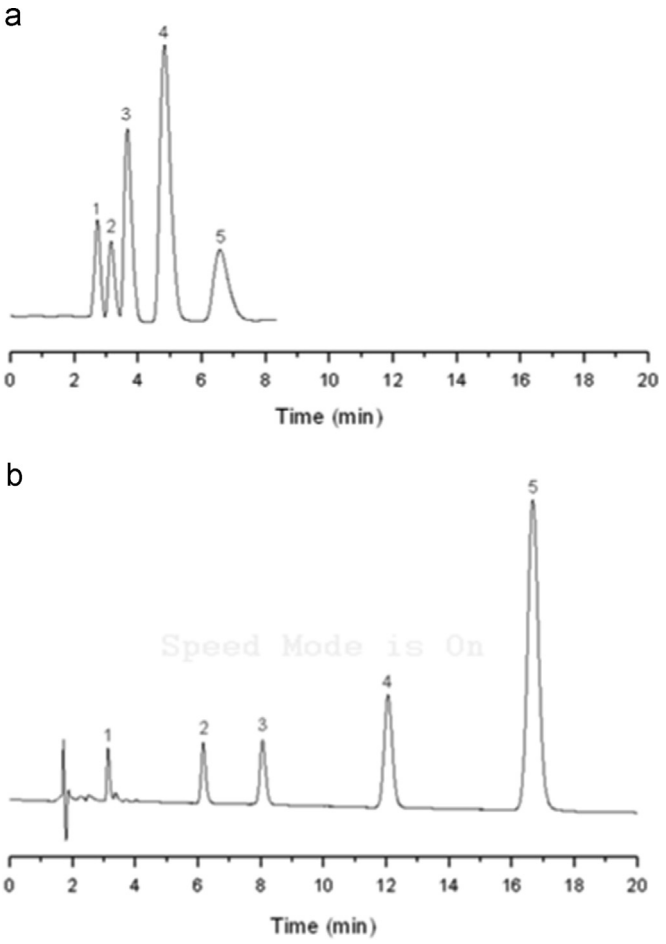

Fig. 2. Chromatograms of PAHs on (**a**) L^1AminoSil and (**b**) ODS. Mobile phase, methanol–water (80/20, v/v); flow rate, 0.8 mL min^{-1}; detection wavelength, 254 nm; column temperature, 30 °C. Peaks: 1, benzene; 2, biphenyl; 3, phenanthrene; 4, chrysene; 5, perylene.

Table 1
The log $K_{o/w}$ values of analytes studies [15].

Analytes	Log $K_{o/w}$
Benzene	2.13
Biphenyl	4.01
Phenanthrene	4.57
Chrysene	5.81
Perylene	5.82
***o*-Cresol**	1.95
Hydroquinol	0.59
Phenol	1.46
2-Naphthol	2.70
3-Nitrophenol	1.91

For nitroaniline, the HPLC condition was optimized to obtain better separation results by comparing with their separation on previous Fc–SiO_2 column. The two cyclopentadienyl carbon rings of ferrocene were hydrophobic and abundant of π-electron, while the –NO_2 substituted group was strong electron withdrawing group. Therefore, hydrophobic, π–π as well as π-electron transfer interactions were responsible for the chromatographic behavior of nitroaniline isomers. As can be seen from Table 2, when L^1AminoSil column was compared with Fc–SiO_2 column, the –NO_2

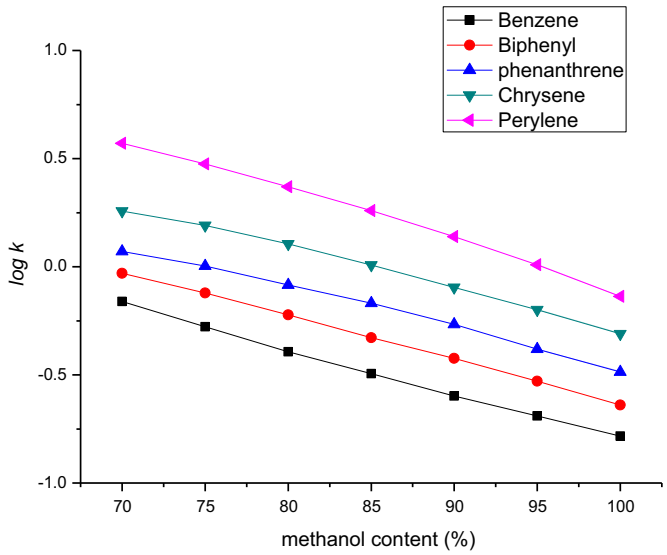

Fig. 3. Effect of methanol content on log k of PAHs on L[1]AminoSil column. Mobile phase, different methanol contents; flow rate, 0.8 mL min^{-1}; detection wavelength, 254 nm; column temperature, 30 °C.

Table 2
The capacity factors (k) of positional isomers on L[1]AminoSil and Fc–SiO_2.

Analytes	L[1]AminoSil[a]			Fc–SiO_2[a]		
	k	α	R	k	α	R
o-Nitroaniline	1.23	–	–	1.84	–	–
m-Nitroaniline	2.29	1.87	2.99	11.56	1.24	0.34
p-Nitroaniline	4.02	1.76	4.40	9.36	5.08	1.27
	L[1]AminoSil[b]			Fc–SiO_2[b]		
	k	α	R	k	α	R
α-Naphthylamine	1.76	–	–	1.33	–	–
β-Naphthylamine	2.28	1.30	1.38	1.97	1.48	1.20
o-Xylene	0.30	–	–	0.30	–	–
m-Xylene	0.30	–	–	0.30	–	–
p-Xylene	0.30	–	–	0.30	–	–
Aniline	0.27	–	–	0.16	–	–
N-Methyl aniline	0.6	2.24	2.4	0.44	2.81	2.34
N, N-dimethyl aniline	1.49	2.49	3.46	1.01	2.31	2.49

[a] Mobile phase: Hexane–isopropanol (70/30, v/v); flow rate, 0.8 mL min^{-1}; detection wavelength, 254 nm; column temperature, 30 °C.
[b] Mobile phase: Hexane–isopropanol (80/20, v/v); flow rate, 0.8 mL min^{-1}; detection wavelength, 254 nm; column temperature, 30 °C.

substituted benzene had shorter retention times on L[1]AminoSil than that on Fc–SiO_2, which might be associated to weaken hydrogen bonding interactions between the L[1]AminoSil and the analytes with the increase of carbonyl numbers and the growth of carbonyl spacer arm. In addition, the elution orders of the three positional isomers were quite different from each other. Fig. 4 showed the typical chromatograms for *o*, *m*, *p*-nitroaniline on both the columns. Obviously, the elution order on L[1]AminoSil was $o < m < p$, which was in agreement with the dipole moment values of nitroaniline increasing from 4.38, 4.91, 6.33 for *o*-, *m*-, *p*-nitroaniline. In contrast to this, the order was $o < p < m$ on Fc–SiO_2. In addition, the chromatographic peak of *m*-nitroaniline was as good as the ones of *o*- and *p*-isomers on L[1]AminoSil, while it gave tailing peak shape on Fc–SiO_2 phase. This was presumably due to the weakly polar of mobile phase in NP mode, which permitted *m*-nitroaniline to interact more favorably with carbonyl group present on the Fc–SiO_2 column. However, multiple interactions might contribute to the chromatographic process of nitroaniline on the ferrocene packing material besides π–π, hydrophobic and

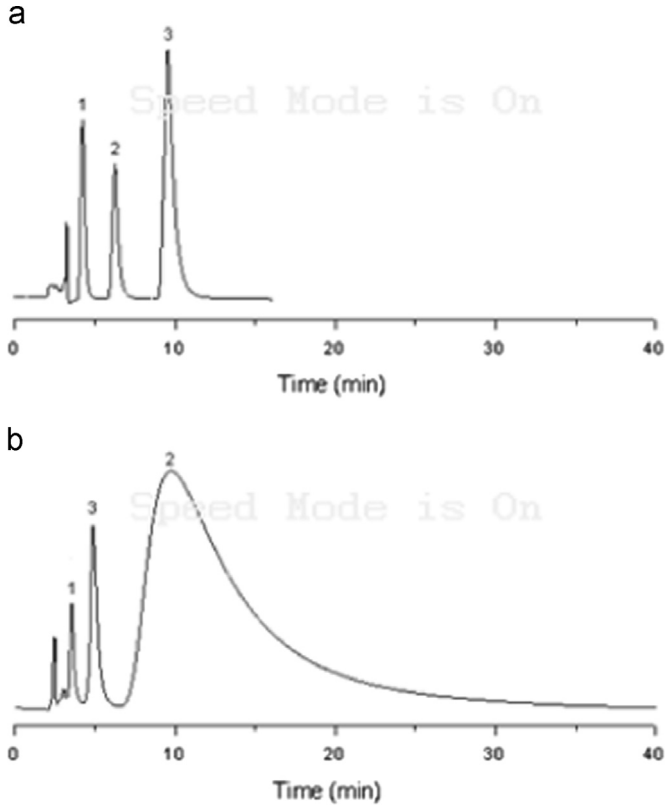

Fig. 4. Chromatograms of *o*-, *m*-, *p*-nitroaniline on (**a**) L[1]AminoSil and (**b**) Fc–SiO_2. Mobile phase: (**a**) hexane–isopropanol (70/30, v/v); flow rate, 0.8 mL min^{-1}; detection wavelength, 254 nm; column temperature, 30 °C. (**b**) hexane–isopropanol (30/70, v/v); flow rate, 0.8 mL min^{-1}; detection wavelength, 254 nm; column temperature, 30 °C. Peaks: 1, *o*-nitroaniline; 2, *m*-nitroaniline; 3, *p*-nitroaniline.

π-electron transfer interactions. It was proposed that the hydrogen bonding interaction might be one of the most important factors playing roles in the retention of *m*-nitroaniline.

From Table 2, it can be seen that positional isomers were well separated except xylene isomers. Because nonpolar xylene position isomers contained nonpolar substituted group CH_3, and had the similar hydrophobicity and π–π interaction with L[1]AminoSil, three xylene position isomers could not be separated from each other. The result was similar to those obtained on Fc–SiO_2 column, which may be the general character of ferrocene stationary phase. Therefore, it is noteworthy that the presence of polar groups such as NO_2 and NH_2 in the aromatic probes might tune the separation selectivity on L[1]AminoSil stationary phase.

3.2.3. *Separation of 5-nitroimidazoles drugs*

Nitroimidazole drugs (5-nitroimidazoles), a kind of broad-spectrum antimicrobials, are widely used in animal husbandry for the treatment of livestock protozoan infection, which can promote the growth of livestock [16,17]. But nitroimidazoles and the metabolites produced have teratogenic, carcinogenic and mutagenic effects on mammals [18,19]. Separation of five nitroimidazole drugs, including rpronidazole, ornidazole, metronidazole, ronidazole and tinidazole, were examined on L[1]AminoSil column. Figs. 5 and 7 show the typital chromatograms of the five nitroimidazole drugs on L[1]AminoSil column with acetonitrile (100%) and 72/18/10 (v/v/v) hexane/isopropyl alcohol/methanol using isocratic mobile phase, respectively. A comparative study was carried out on ODS stationary phase under the same chromatographic conditions in reversed-phase mode (Fig. 5). Obviously, on ODS phase the co-elution of the five drugs were observed. But the five nitroimidazoles can be effectively separated on L[1]AminoSil

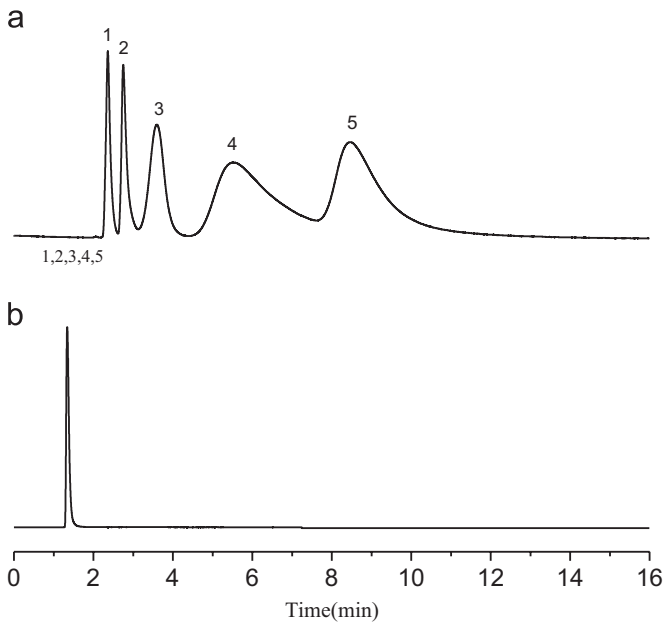

Fig. 5. Chromatograms of nitroimidazole drugs on (**a**) L[1]AminoSil and (**b**) ODS. Mobile phase: acetonitrile (100%); flow rate, 0.8 mL min^{-1}; detection wavelength, 320 nm; column temperature, 30 °C. Peaks: 1, rpronidazole; 2, tinidazole; 3, ronidazole; 4, ornidazole; 5, metronidazole.

column in RP-HPLC and NP-HPLC. L[1]AminoSil phase exhibited the highest retention power and selectivity towards such analytes.

Methanol and acetonitrile are the most common organic modifiers of mobile phase in RP-HPLC. Methanol has stronger H-bonding donating ability and less lipophilicity than acetonitrile. Acetonitrile is an electron rich organic modifier, which could suppress the π–π interactions between the analyte and the stationary phase. The selectivity and retention behaviors of L[1]AminoSil could be influenced using different organic modifiers owing to different adsorptions of the organic modifier on the adsorbent surface [20]. As shown in Fig. 6, with increasing acetonitrile content in the aqueous eluent the retentions of nitroimidazole increased. The effect of small changes in the mobile phase on log *k* was significant. The L[1]AminoSil phase seems to show hydrophilic interaction chromatographic mode using

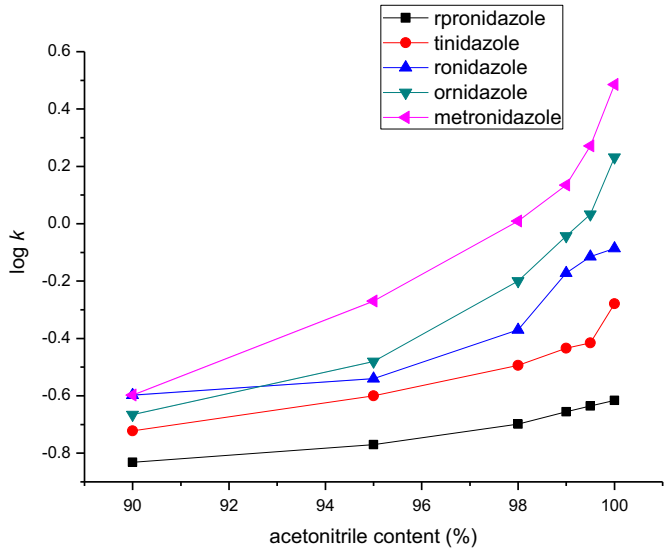

Fig. 6. Effect of acetonitrile content on the retention of 5-nitroimidazoles drugs. Mobile phase: different acetonitrile contents in water; flow rate, 0.8 mL min^{-1}; detection wavelength, 320 nm; column temperature, 30 °C.

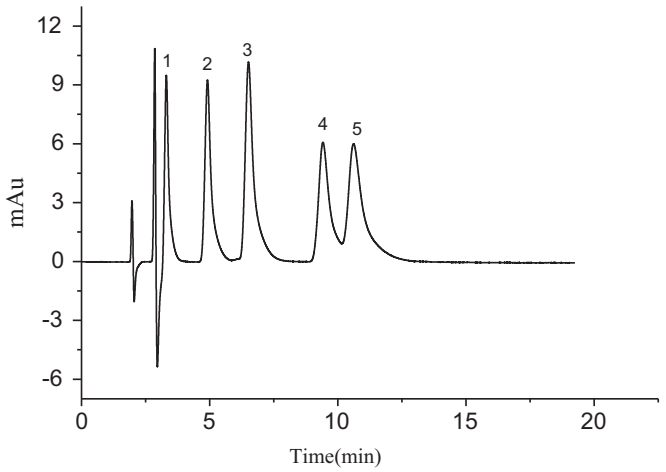

Fig. 7. Chromatograms of nitroimidazole drugs on L[1]AminoSil column. Mobile phase: hexane/isopropyl alcohol/methanol (72/18/10, v/v/v); flow rate, 0.8 mL min^{-1}; detection wavelength, 320 nm; column temperature, 30 °C. Peaks: 1, rpronidazole; 2, ornidazole; 3, metronidazole; 4, ronidazole; 5, tinidazole.

acetonitrile as organic modifier, and five compounds could be separated when pure acetonitrile served as the elution condition. It could be deduced that the hydrophilic interaction might be responsible for the retention in RP mode.

L[1]AminoSil may interact with nitroimidazole drugs by dipole–dipole and hydrogen bonding interactions, which were expected to enhance the selectivity of the new phase for analytes in NP-HPLC. As shown in Fig. 7 and Table 3, the baseline separation of five drugs including rpronidazole, ornidazole, metronidazole, ronidazole and tinidazole could be achieved.

3.2.4. Separation of organophosphorus pesticides

L[1]AminoSil column was applied for the separation of organophosphorus pesticides including profenofos, phoxim, pyrazophos, parathion-methyl. Fig. 8 show the typical chromatograms of organophosphorus pesticides on L[1]AminoSil column in normal-phase (NP) mode. In NP-HPLC, the baseline separation of four organophosphorus pesticides could be obtained in 8 min and parathion-methyl was eluted finally. The charge-transfer interaction resulting from nitro group of last analyte was responsible for the increase in retention of parathion-methyl. It was confirmed again that the retention mechanism of the new stationary phase in NP-HPLC was ascribed to multi-interaction, like π–π, dipole–dipole as well as charge-transfer interactions, which resulted in the change of selectivity of L[1]AminoSil column for different types of solutes. In comparison with NP condition, although above-mentioned polar interactions were involved in the retention, four organophosphorus pesticides had similar retention (Table 3) and could not be separated in RP-HPLC.

3.2.5. Separation of phenols

The unique structure of the attached ferrocene molecule provided a multi-mode retention mechanism for solutes and might offer the possibility of strong interactions with phenols. To demonstrate the special selectivity and retention mechanism of L[1]AminoSil for phenols, five representative phenols including hydroquinol, phenol, 3-nitrophenol, *o*-cresol and 2-naphthol were used for the evaluation. The retention factors of phenols were listed in Table 3 under different chromatographic conditions. The elution order of compounds on L[1]AminoSil phase was not in agreement with that on ODS phase [21] in RP-HPLC. The retention of phenols increased with their hydrophobicity except *o*-cresol and 3-nitrophenol (the log $K_{o/w}$ values were listed in Table 1). Solutes were firstly separated according to their hydrophobicity as usual in

Table 3
Comparison of k, α and R of analytes between RP- and NP-HPLC.

	RP-HPLC[a]			NP-HPLC[b]		
	k	α	R	k	α	R
Benzene	0.43	–	–	0.21	–	–
Biphenyl	0.66	1.52	1.91	0.27	1.23	0.56
Phenanthrene	0.93	1.41	2.09	0.42	1.56	1.56
Chrysene	1.43	1.55	3.07	0.64	1.52	1.78
Perylene	2.45	1.71	4.46	1.00	1.56	1.88
	RP-HPLC[c]			NP-HPLC[d]		
	k	α	R	k	α	R
rpronidazole	0.24	–	–	0.66	–	–
Omidazole	1.71	2.08	2.23	1.46	2.21	1.51
Metronidazole	3.06	1.79	2.40	2.28	1.56	2.40
Ronidazole	0.82	1.56	1.55	3.74	1.64	3.54
Tinidazole	0.53	2.17	2.45	4.34	1.16	1.14
	RP-HPLC[e]			NP-HPLC[f]		
	k	α	R	k	α	R
Profenofos	0.41	–	–	0.39	–	–
Phoxim	0.41	–	–	0.93	2.38	4.00
Pyrazophos	0.41	–	–	1.54	1.66	2.42
Parathio-methyl	0.41	–	–	2.42	1.35	2.07
	RP-HPLC[g]			NP-HPLC[h]		
	k	α	R	k	α	R
o-Cresol	0.37	–	–	0.64	–	–
Phenol	0.56	1.27	0.79	0.88	1.38	0.98
2-Naphthol	0.88	1.57	1.10	1.24	1.41	1.04
p-Dihydroxybenzene	0.44	1.19	0.51	2.00	1.61	1.25
3-Nitrophenol	1.40	1.59	1.10	5.33	2.67	4.40

[a] Methanol–water (80/20, v/v); flow rate, 0.8 mL min^{-1}; detection wavelength, 254 nm; column temperature, 30 °C.
[b] Hexane–isopropanol (95/5, v/v);; flow rate, 0.8 mL min^{-1}; detection wavelength, 254 nm; column temperature, 30 °C.
[c] Acetonitrile (100%); flow rate, 0.8 mL min^{-1}; detection wavelength, 320 nm; column temperature, 30 °C.
[d] Hexane/isopropyl alcohol/methanol (72/18/10, v/v/v); flow rate, 0.8 mL min^{-1}; detection wavelength, 320 nm; column temperature, 30 °C.
[e] Methanol–water (98/2, v/v); flow rate, 0.8 mL min^{-1}; detection wavelength, 254 nm; column temperature, 30 °C.
[f] Hexane/isopropyl alcohol (98/2, v/v); flow rate, 0.8 mL min^{-1}; detection wavelength, 254 nm; column temperature, 30 °C.
[g] Acetonitrile/water (95/5, v/v); flow rate, 0.8 mL min^{-1}; detection wavelength, 230 nm; column temperature, 30 °C.
[h] Hexane/isopropyl alcohol/methanol (72/8/20, v/v/v); flow rate, 0.8 mL min^{-1}; detection wavelength, 230 nm; column temperature, 30 °C.

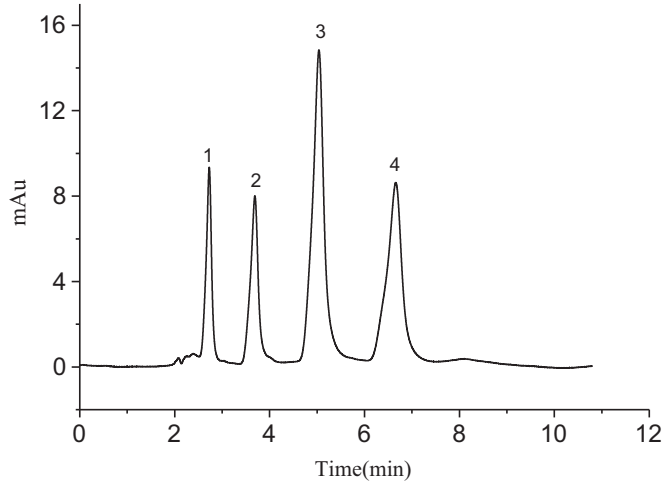

Fig. 8. Chromatograms of organophosphorus pesticides on L^1AminoSil column. Mobile phase: hexane/isopropyl alcohol (98/2, v/v); flow rate, 0.8 mL min^{-1}; detection wavelength, 254 nm; column temperature, 30 °C. Peaks: 1, profenofos; 2, phoxim; 3, pyrazophos; 4, parathio-methyl.

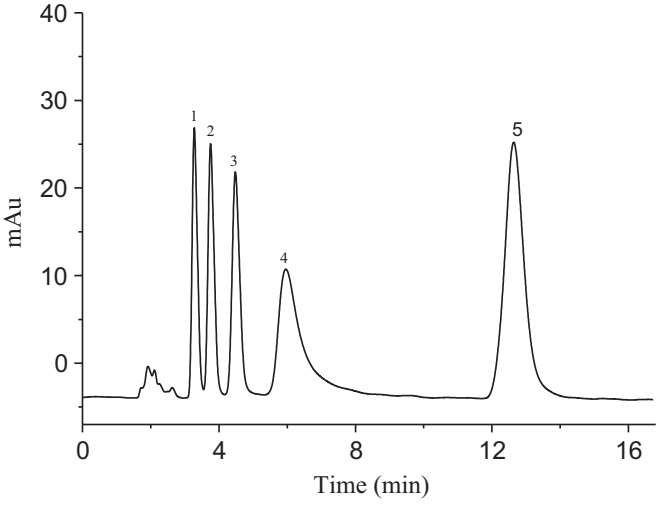

Fig. 9. Chromatograms of phenols on L^1AminoSil column. Mobile phase: hexane/isopropyl alcohol/methanol (72/8/20, v/v/v); flow rate, 0.8 mL min^{-1}; detection wavelength, 230 nm; column temperature, 30 °C. Peaks: 1, *o*-cresol; 2, phenol; 3, 2-naphthol; 4, hydroquinol; 5, 3-nitrophenol.

typical RP-HPLC. The strongest retention of L^1AminoSil column for 3-nitrophenol, as compared with ODS column, was likely due to the fact that the acid–base equilibrium between the hydroxy group of 3-nitrophenol and the amino group of L^1AminoSil played a significant role. The existence of electron-attracting group ($-NO_2$) causes the formation of acid–base equilibrium between the hydroxy group of nitrophenol and amino group of L^1 molecule. In comparison with 3-nitrophenol, *o*-cresol was likely to form weaker acid–base equilibrium interaction with amino groups on L^1AminoSil packing because of electrondonating substituent ($-CH_3$), which could be the reason why it was eluted firstly.

The acid–base equilibrium could be also confirmed by the fact that 3-nitrophenol eluted finally among above five analytes in NP-HPLC (Fig. 9). The retention of 2-naphthol on L^1AminoSil in NP-HPLC did not correspond with the polarity, which was due to the π–π interaction enhancing its retention. Besides above mentioned interactions, hydrogen bonding and dipole–dipole interactions were responsible for the retention of solutes in NP-HPLC. According to the selectivity factor (α) of L^1AminoSil for five phenols in Table 3, L^1AminoSil in NP-HPLC showed higher selectivity for the *o*-cresol and phenol pair as well as the 2-naphthol and hydroquinol pair than that in RP-HPLC, thus L^1AminoSil phase could preferably be operated in NP-HPLC to separate the polar phenols.

3.2.6. Determination of organophosphorus pesticide residue in vegetable sample on L^1AminoSil column

Organophosphorus pesticides have been widely used in agriculture throughout recent decades to ensure a supply of food for the world's growing population. However, adverse effects of this use can be seen in the chemical residues found in food. But neuroinhibitors such as organophosphorus pesticides display a high acute toxicity in humans [22]. Consequently, there is a growing interest in fast and more sensitive detection systems [23–28]. Also in this paper, we try to develop the rapid analysis of oganophosphorus pesticides in vegetable sample by simple HPLC method on L^1AminoSil column.

The cowpea sample smashed by soymilk machine was treated with acetonitrile and NaCl to dissociate the target analyte from the sample matrix. The mixed solution was centrifuged and the supernatant was applied to an Aligent NH_2 SPE column clean up.

The linearity of phoxim, pyrazophos, parathio-methyl was satisfactory in the range of 0.1–20 μg/mL. Under the optimal conditions, the linearity equations, regression coefficients R^2, limits of

Table 4
The linearity equation, R^2, LOD and LOQ of three organophosphorus pesticides on L[1]AminoSil column.

Analyte	Phoxim	Pyrazophos	Parathio-methyl
Linearity equation	$y=21184.3\ x-616.9$	$y=138473.2\ x-581.7$	$y=88546.1\ x+102.3$
Regression coefficient R^2	0.9998	0.9990	0.9997
LOD (μg/mL)	0.020	0.031	0.029
LOQ (μg/mL)	0.12	0.20	0.19

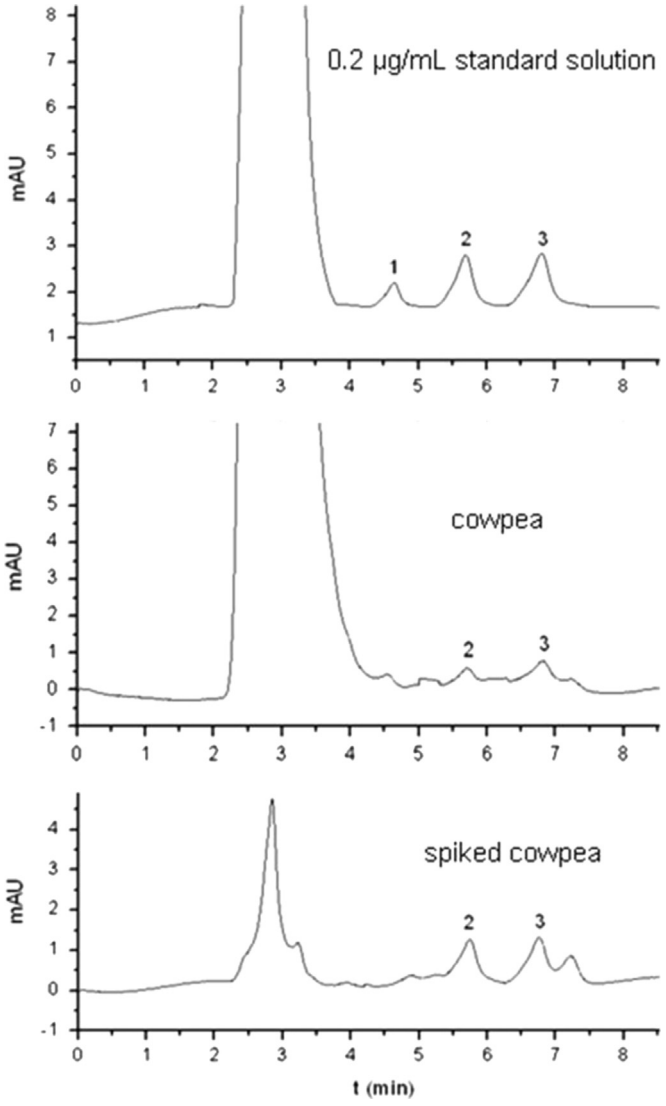

Fig. 10. Chromatogram of three organophosphorus pesticides in cowpea on L[1]AminoSil column. Mobile phase: hexane/isopropyl alcohol (98/2, v/v); flow rate, 0.7 mL min^{-1}; detection wavelength, 254 nm; column temperature, 30 °C. Peaks: 1, phoxim; 2, pyrazophos; 3, parathio-methyl.

detection (LOD) and limits of quantitation (LOQ) were listed in Table 4. The RSD% values of retention times and peak areas in intra- and inter-day assays for these pesticides were all below 0.15% and 0.16%, which showed good precision and accuracy. The recoveries of phoxim, pyrazophos, parathio-methyl for cowpea sample spiked with 0.5 μg/mL and 2.0 μg/mL were in the range of 92–98%, 91–103% and 93–99% with the RSDs less than 1.6% ($n=6$), 2.3% ($n=6$) and 1.6% ($n=6$), respectively. The optimized chromatogram of phoxim, pyrazophos, parathio-methyl on an L[1]AminoSil column was shown in Fig. 10, from which we can see that three organophosphorus pesticides obtained better separation from the matrix. The residues of pyrazophos, parathio-methyl in cowpea were 13.2 μg/kg and 9.7 μg/kg, respectively. But phoxim was not detected.

4. Conclusions

The new promising stationary phase based on L[1] AminoSil was prepared in this paper. Characterization using infrared spectroscopy, elemental analysis and thermogravimetric analysis proved that this ferrocene molecule was covalently attached on the silica surface. The L[1]AminoSil phase could provide various action sites including hydrophobic, dipole–dipole, π–π, hydrogen bonding interactions and acid–base equilibrium and presented a multi-mode retention mechanism for different types of analytes. Simultaneous interactions enabled the new phase to be operated in RP- and NP-HPLC with excellent chromatographic properties. To some extent, the L[1]AminoSil phase showed prospect for the separation of neutral aromatic compounds, aromatics positional isomers, 5-nitroimidazole drugs, polar pesticides and phenols. Three organophosphorus pesticides and vegetable matrix could be baseline separated within 8 min on L[1] AminoSil column.

Acknowledgments

The authors acknowledge the support of NSF of China (21205107, 21275133, 21475119) for financial support of this research.

Appendix A. Supplementary material

Supplementary data associated with this article can be found in the online version at http://dx.doi.org/10.1016/j.talanta.2015.07.063.

References

[1] D. Harrison, I. Coulter, S. Wang, S. Nistala, B. Kuntz, M. Pigeon, J. Tian, S. Collins, J. Mol. Catal. A 128 (1998) 65.
[2] M. Mifune, T. Kanai, M. Urabe, A. Iwado, J. Haginaka, N. Motohashi, Y. Saito, Anal. Sci. 15 (1999) 581.
[3] M. Mifune, M. Onoda, T. Takatsuki, T. Kanai, A. Iwado, N. Motohashi, J. Haginaka, Y. Saito, Chem. Pharm. Bull. 47 (1999) 346.
[4] J. Xiao, C. Kibbey, D. Coutant, G. Martin, M. Meyerhoff, J. Liq. Chromogr. Rel. Technol. 19 (1996) 2901.
[5] E. Lindner, A. Baumann, P. Wegner, H. Mayer, U. Reinohl, A. Wever, T. Ertel, H. Bertagnolli, Mater. Chem. 10 (2000) 1655.
[6] O. Bordelanne, M. Delville, Solid State Sci. 4 (2002) 851.
[7] O. Bordelanne, M. Delville, G. Felix, C. Labrugere, A. Thienpont, C. Vidal, Chromatographia 52 (2000) 51.
[8] Q. Huai, X. Wang, Y. Zuo, Chromatographia 55 (2002) 549.
[9] Q. Huai, J. You, Q. Wang, Y. Zuo, Chromatographia 57 (2003) 709.
[10] A. Yu, D. Peng, K. Hu, A. Cao, J. Chang, Y. Wu, S. Zhang, J. Chromatogr. A 1283 (2013) 75.
[11] M. Sliwka-Kaszynska, S. Karaszewski, J. Sep. Sci. 31 (2008) 926.
[12] M. Barc, M. Sliwka-Kaszynska, J. Chromatogr. A 1216 (2009) 3954.
[13] C. Schneider, T. Jira, J. Chromatogr. A 1216 (2009) 6285.
[14] J. Gallagher, P. Kenny, M. Sheehy, Inorg. Chem. Commun. 2 (1999) 327.
[15] C. Hansch, A. Leo, D. Hoekman, Exploring QSAR-hydrophobic, electronic and steric constants, Am. Chem. Soc., 1995.
[16] M. Hernandez-Mesa, D. Airado-Rodriguez, C. Cruces-Blanco, A. Garcia-Campana, J. Chromatogr. A 1341 (2014) 65.
[17] N. Mallo, J. Lamas, J. Leiro, Antimicrob. Agents Chemother. 57 (2013) 2476.
[18] M. Hernandez-Mesa, C. Cruces-Blanco, A. Garcia-Campana, Anal. Bioanal. Chem. 404 (2012) 297.
[19] C. Williams, D. Lloyd, D. Kolarich, K. Alagesan, M. Duchene, J. Cable, D. Williams, D. Leitsch, Vet. Parasitol. 190 (2012) 62.
[20] F. Chan, L. Yeung, R. LoBrutto, Y. Kazakevich, J. Chromatogr. A 1082 (2005) 158.
[21] D. Xuan, Y. Li, China Public Health 18 (2002) 1102.

[22] L. Karalliedde, H. Wheeler, R. Maclehose, V. Murray, Public-Health 114 (2000) 238.
[23] A.I. Valenzuela, R. Lorenzini, M.J. Redondo, G. Font, J. Chromatogr. A 839 (1999) 101.
[24] H. Schulze, R.D. Schmid, T.T. Bachmann, Anal. Bioanal. Chem. 372 (2002) 268.
[25] C. García-Ruiz, G. Llamas, A. Puerta, E. Blanco, A. Sanz-Medel, M.L. Marina, Anal. Chim. Acta 543 (2005) 77.
[26] M. Hamada, R. Wintersteiger, J. Planar Chromatogr.—Mod. TLC 16 (2003) 4.
[27] D. Chen, J.J. Wang, Y. Xu, D.H. Li, L.Y. Zhang, Z.X. Li, Biosens. Bioelectron. 41 (2013) 163.
[28] K. Prasad, K.P. Prathish, J.M. Gladis, G.R. Naidu, T.P. Rao, Electroanalysis 19 (2007) 1195.